Optica Applicata, Vol. XXIII, No. 1, 1993

Simplified interference measurement of the refractive index distribution in the slices of preforms and waveguides. Destructive method of plane reference wave and some of its variants

W. Kowalik

Institute of Physics, Technical University of Wrocław, Wybrzeże Wyspiańskiego 27, 50-370 Wrocław, Poland.

A simplified interference measurement method of refractive index distribution in slices of both preforms and light waveguides is presented. Different variants simplifying the measurement were described. The measurement errors introduced by the accepted simplifications were analysed. Also, the interference measurement methods for determination of the refractive index differences between the coat of either preform or waveguide and the immersion liquid are described. A simplified method of thickness distribution in the given slice is presented. The proposed destructive measurement methods may serve as a controlling pattern for the nondestructive methods.

1. Problems associated with the typical assumptions of the nondestructive interference methods

In the course of elaborating the nondestructive interference methods there appeared the problem of measurement accuracy estimation [1]–[9]. When analysing these accuracies numerous questions were to be answered to make the analysis both complete and unique. The purpose of this work is to answer some of these questions.

Many nondestructive interference methods are based on the measurements during which the object is located in a cuvette filled with an immersion liquid of the refractive index equal to refractive index of the coat of the object examined (Fig. 1). Such a procedure is justified since it makes the measurement result independent of both the geometry and the refractive index value of the coat as well as simplifies the calculations. Some of the methods do not require the equality of the said refractive indices but they are charged with an error introduced by the deviation of the coat geometry from the cylindric form.

When a plane wavefront g_0, emerging from a collimator, passes through the examined object, the deformation of this front due to nonuniformities of the core (measured with respect to the nonperturbed front passing through the coat of the examined object) is equal to [7], [8]

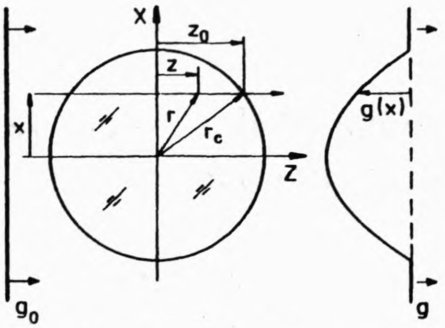

Fig. 1. Transition of the plane wave through a nonuniform core

$$\delta g(x) = 2\int_{0}^{z_0} \delta n(r)dz. \tag{1}$$

This is valid under assumption that the refractive index distribution in the core changes in a continuous way and is the function of the radius r only (Fig. 1), while $z = \sqrt{r^2 - x^2}$. The function $\delta n(r)$ is a difference of the refractive index distribution in the core $n(r)$ and the refractive index n_c of the coat of the examined object. The difference operator is δ. After having changed the integration variables in (1) the shape of the relative wavefront is given in the form

$$\delta g(x) = 2\int_{x}^{r_c} \frac{\delta n(r) r\, dr}{\sqrt{r^2 - x^2}}, \tag{2}$$

while after having applied the Abel transformation, the relative distribution of the refractive index is obtained

$$\delta n(r) = -(1/\pi)\int_{r}^{r_c} \frac{[d(\delta g(x))/dx]dx}{\sqrt{x^2 - r^2}}. \tag{3}$$

As we see, the spatial distribution of the refractive index may be determined by exploiting the information about the one-dimensional wavefront $g(x)$. But for this purpose the following assumptions must be made:

1. The core and the coat are of cylindric symmetry and are concentric.
2. The refractive index in the core is a function of the radius r only.
3. The refractive index in the core is a continuous and smooth function.

However, it is known from practice, that these assumptions are never fulfilled completely. Therefore, the question must be answered of how great the deviation is in each case and how it influences the measurement result. This is especially essential when analysing the measurement accuracies for the nondestructive methods. The answer to this question may be found by comparing the results offered by the nondestructive method with those given by the destructive one; the destructive method [10] being considered as a standard for the nondestructive one.

The following goals should be achieved in this work:

i) Elaboration of the destructive measurement method and performing of the measurements of the real distribution of the refractive index in the slices of optical preforms for the case of surveying the slices along the preform axis. Only the destructive method enables the measurement of the real distribution of the refractive index.

ii) Measurement of the geometry of the examined objects (core and layers in the core).

The measurements of geometry should give the answer to the following questions:

1. What are the maximal and typical deformations of the core?

2. Do the deformations of the external part of the core convey to all the layers in the core?

The measurements of the refractive index distribution (together with geometry measurements) should give the answer to the questions:

1. How do the measurement results of the refractive index distribution correspond to refractive index profile obtained from the nondestructive method?

2. What are the maximal and typical errors of the nondestructive method?

3. Is it possible to increase the accuracy of the nondestructive method and to what degree by taking account of the core deformation (its ellipticity, for instance).

In the present paper only the destructive method is presented. The partial answers to the other questions are available in the works concerning the measurement errors of the nondestructive method [1], [2], [4]–[6], [11]–[14].

In the work [15], a very accurate method allowing us to measure the refractive index distribution as well as the thickness distribution in the phase objects was discussed. The method requires the production of three interferograms, and it is unnecessary to insert the object in an immersion cuvette. In practice, not always a very high measurement accuracy is required. In this work, some simplified methods have been analysed for which two or just one interferogram are produced. The given ways of simplifying the related formula allow us to reduce significantly the number of data subject to the analysis, with simultaneous knowledge of the increase of the measurement error associated with such simplification. In the measuremental practice, especially when the number of the measurements to be performed is great, the measurement simplification becomes both important and justified economically. The given versions of the simplified measurements concern the preform and waveguide slices. By the suitable slight modifications, however, they may be easily adjusted to the examination of other phase objects.

2. Interference measurements of the refractive index distribution in slices – destructive method

2.1. Measurement setup

The measurements are performed in a Mach–Zehnder interferometer adjusted to the observation of fringes of equal thickness. The light source is a He-Ne laser ($\lambda = 632.8$ nm). The collimator produces at its exit a broadened parallel beam of

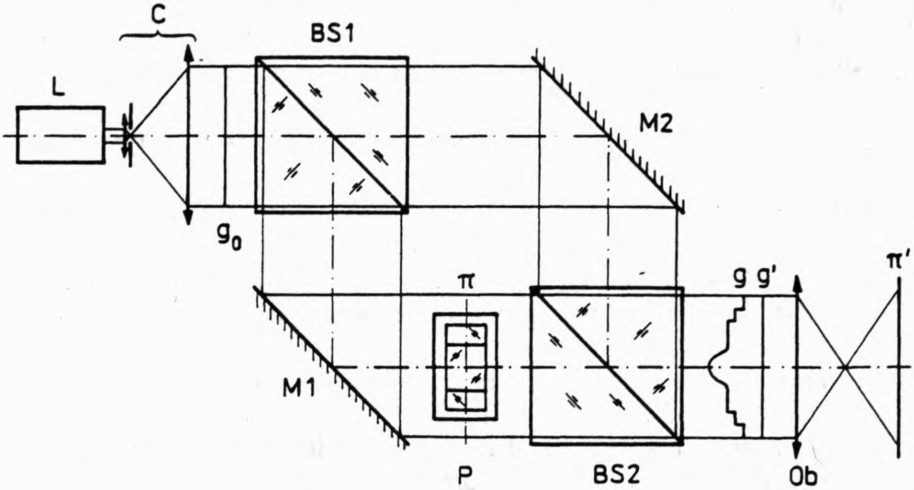

Fig. 2. Mach–Zehnder interferometer for measurement of the refractive index distribution in the slice of preforms or optical waveguides. L – laser, C – collimator, BS1 and BS2 – beam splitters, M_1 and M_2 – mirrors, P – sample slice located in the immersion cuvette, Ob – objective imaging the slice Π in the plane Π'. The wavefront g_0, after having passed through both arms of the interferometer, gives two wavefronts g and g'

plane wavefront g_0 (Fig. 2)). This beam is split at the first beam splitter BS1. The first of the split beams passes through the BS1–M1–BS2 interferometer arm suffering from deformation when passing through the cuvette containing both the immersion liquid and the examined slice P located in the plane Π. At the exit of the interferometer arm a deformed wavefront g is obtained. The deformation of the wavefront depends on the distribution of the refractive index in the slice of the examined object and the slice thickness distribution. The slice is transilluminated along the symmetry axis of the core. The other (reference) beam is transmitted along the BS1–M2–BS2 interferometer arm and reaches the objective Ob as a wavefront g'. The refractive index distribution in the core is measured with respect to the refractive index of the coat of the examined object. The objective Ob images the slice P in the plane Π'. The latter may be the object plane for the eypiece (in the case of immediate observation) or the plane of the film of a photocamera or the detection plane of a TV CCD camera connected with a computer (IBM with Frame Grabber, for instance).

The interferograms (static images with interference fringes) are subject to scanning during which the position x of the interference fringes, *i.e.* that of the orders $m(x)$ on the scanning lines is determined. The interference orders being the numbers of the fringes are the whole numbers. In the case of relative measurements, as it happens for majority of interference measurements, the relative values of the interference orders (differences of orders) are needed rather than their absolute values. It is most important to know in which direction the orders increase. This is determined by observing the dynamic fringes (during regulation of the interferometer mirrors). The orders increase in the direction from the optical wedge

edge. The edge of the wedge is a place in which the dynamic fringes converge (during the motion of the mirror) when the distance between the moving fringes diminishes. The analysis of the interferogram consists in performing an approximation of the $m(x)$ function defined on the set of sampling data which provide the information about the orders and their positions on the scanning line in order to find the analytic function $m(x)$.

2.2. Principle of measurement

In order to choose a suitable measurement method and determine the errors associated with the simplifying assumptions two interferograms will be considered.

The first interferogram **1** was produced in the setup from Fig. 2 where a slice of the examined object is located in the cuvette with the immersion liquid. The second interferogram **2** was produced in the same setup with the same immersion cuvette but without the examined object. On the interferogram **1**

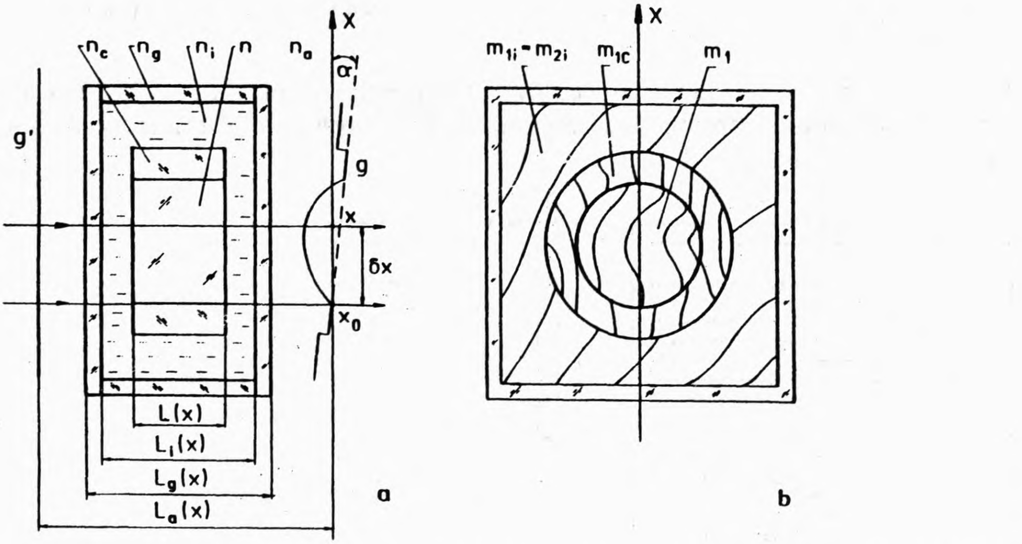

Fig. 3. Interferogram **1**. **a** "longitudinal" section through the cuvette with the slice (the refractive indices and thicknesses of the due media are marked), **b** – "transversal" section through the cuvette with the slice (the regions of three structures of fringes are presented)

(Fig. 3) the optical path difference between the wavefronts g and g' encoded in the form of interference orders $m_1 = (g-g')/\lambda$ is determined. The front g represents the deformations introduced by the first arm of the interferometer, the immersion cuvette and the examined object. The wavefront g' represents the deformations caused by the second arm of the interferometer. In contrast to this on the interferogram **2** (Fig. 4), the optical path difference between the wavefronts g'' and g' is recorded being encoded in the form of the interference orders $m_2 = (g''-g')/\lambda$, where g'' is the wavefront emerging after the plane wave g_0 have passed through the first arm of the interferometer with an immersion cuvette but without the examined object (slice).

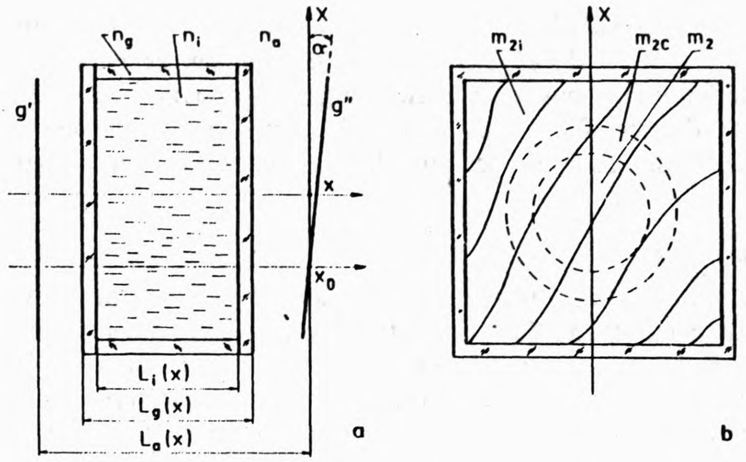

Fig. 4. Interferogram 2. a — "longitudinal" section through the cuvette (the refractive indices and thicknesses of the due media are marked), b — "transversal" section through the cuvette (the regions of single fringe structure are marked)

Both the interferograms are produced while the position of the mirrors M_1 and M_2 is unchanged (after recording the interferogram 1 the position of the mirrors M_1 and M_2 remains the same).

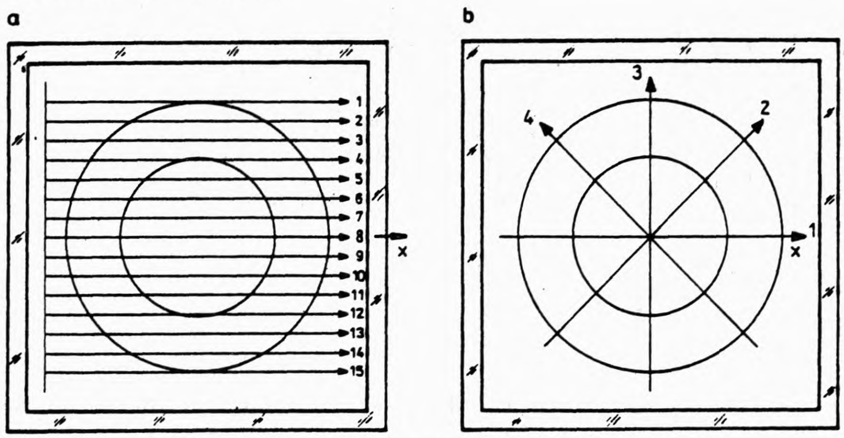

Fig. 5. Systems of interferogram scanning. a — parallel scanning lines , b — scanning lines for radial system

The interference orders recorded on interferograms are two-dimensional. During the analysis of such interferogram the whole interferogram is covered by the scanning lines (Fig. 5). The further dependences describe the one-dimensional relations (x-direction) which are true for any scanning lines.

In order to obtain a quantitative description of the phenomena the following reasoning has been carried out. From the whole beam passing through the cuvette with immersion liquid (and eventually with the examined sample) two rays are separated. The current scanning ray passes through the running point x on the interferogram, while the reference scanning ray – through the reference point x_0 with respect to which the magnitudes n, m_1, m_2, L, L_i, L_g, L_a ... (Fig. 3) are measured. The difference (operator of changes) of the corresponding magnitudes of the coordinates x and x_0 is denoted by δ (for instance, $\delta n(x) = n(x) - n(x_0)$).

Interferogram 1 (produced in an interferometer with the examined object in the cuvette). The optical path differences for two rays are:

$$[L_a(x) - L_g(x)]n_a + [L_g(x) - L_i(x)]n_g + [L_i(x) - L(x)]n_i + L(x)n(x) = \lambda m_1(x),$$

and

$$[L_a(x_0) - L_g(x_0)]n_a + [L_g(x_0) - L_i(x_0)]n_g + [L_i(x_0) - L(x_0)]n_i + L(x_0)n(x_0) = \lambda m_1(x_0), \tag{4}$$

respectively, where m is the interference order, n_a, n_g, n_i, $n(x)$ are refractive indices of the respective media, λ is the wavelength of the light in the interferometer. For the interference orders the following notations have been assumed: the first index shows the interferogram number (1 – interferogram with a slice, 2 – interferogram without a slice), the second index (Fig. 3**b**) denotes the area of the domain of the interferogram 1 (without index – core, c – region of the coat, i – region of the immersion liquid). After having subtracted the suitable sides of Eqs. (4), we obtain:

i) In the region of the core

$$\delta L_a(x)n_a + \delta L_g(x)(n_g - n_a) + \delta L_i(x)(n_i - n_g) + \delta L(x)(n(x_0) - n_i) + \delta n(x)[L(x_0) + \delta L(x)] = \lambda \delta m_1(x) \tag{5}$$

where $\delta L_a n_a$ represents the slope of the wavefronts caused by the interferometer itself (*i.e.* by the position of its mirrors).

ii) In the region of the coat

$$\delta L_a(x)n_a + \delta L_g(x)(n_g - n_a) + \delta L_i(x)(n_i - n_g) + \delta L_c(x)(n_c(x_0) - n_i) + \delta n_c(x)[L_c(x_0) + \delta L_c(x)] = \lambda \delta m_{1c}(x). \tag{6}$$

If the coat is uniform ($\delta n_c(x) = 0$), Eq. (6) reduces to the form

$$\delta L_a(x)n_a + \delta L_g(x)(n_g - n_a) + \delta L_i(x)(n_i - n_g) + \delta L_c(x)(n_c - n_i) = \lambda \delta \mathrm{m}_{1c}(x). \tag{7}$$

iii) In the region of immersion

$$\delta L_a(x)n_a + \delta L_g(x)(n_g - n_a) + \delta L_i(x)(n_i - n_g) = \lambda \delta m_{1i}(x). \tag{8}$$

Note that the interferogram 1 has three separate domains of the interference orders (Fig. 3**b**). The most convenient point of reference x_0 is the point at the core–coat border. Let us assume that the continuity of interference orders is preserved, *i.e.* $n(x_0) = n_c(x_0)$ and $L(x_0) = L_c(x_0)$.

Interferogram 2 (produced in an interferometer with cuvette without the examined object).

Writing the differences of optical paths in the way it has been done for the interferogram 1 in the formulae (4), and subtracting suitable sides of Eqs. (4), an equation is obtained being true for the interferogram 2 in three regions: core, coat and immersion.

i) In the core region

$$L_a(x)n_a+\delta L_g(x)(n_g-n_a)+\delta L_i(x)(n_i-n_g) = \lambda\delta m_2(x). \tag{9}$$

ii) In the coat region

$$\delta L_a(x)n_a+\delta L_g(x)(n_g-n_a)+\delta L_i(x)(n_i-n_g) = \lambda\delta m_{2c}(x). \tag{10}$$

iii) In the immersion region

$$\delta L_a(x)n_a+\delta L_g(x)(n_g-n_a)+\delta L_i(x)(n_i-n_g) = \lambda\delta m_{2i}(x). \tag{11}$$

In this case, for the inside of the immersion cuvette the interference orders are continuous and smooth at the borders of those regions and create one system of fringes (Fig. 4b). Note that for the domain of the immersion region the interference orders are the same for both the interferograms 1 and 2, *i.e.* $m_{1i}(x) = m_{2i}(x)$. The left hand sides of Eqs. (9)–(11), described by the orders of interference from the interferogram 2, occur in Eqs. (5)–(8), and describe the influence of the position of the interferometer mirrors, geometric dimensions of the cuvette and the differences of the refractive indices.

The refractive index distribution in the core may be determined by using only the interferogram 1, but it may also be done by using simultaneously the two interferograms 1 and 2. In the first case, from (5) we have

$$\delta n(x) = \frac{\lambda\delta m_1(x)-[\delta L_a(x)n_a+\delta L_g(x)(n_g-n_a)+\delta L_i(x)(n_i-n_g)+\delta L(x)(n(x_0)-n_i)]}{L(x_0)+\delta L(x)}. \tag{12}$$

While, in the other one, we get from (5) and (9)

$$\delta n\,(x) = \frac{\lambda(\delta m_1(x)-\delta m_2(x))-\delta L(x)(n(x_0)-n_i)}{L(x_0)+\delta L(x)} \tag{13}$$

where $n(x_0)$ is the refractive index of the examined object in the point x_0 and $L(x_0)$ is the object thickness in this point. For a uniform coat and continuous orders of interference in the refractive point we have $n(x_0) = n_c$. As continuous orders the interference orders of fringes of continuous distribution in the interferograms will be understood. Note that the formula for $\delta n(x)$ becomes much simpler (13) when using two rather than one interferogram only (12).

If the coat is nonuniform, then from (6) and (10) we have

$$\delta n_c(x) = \frac{\lambda[\delta m_{1c}(x)-\delta m_{2c}(x)]-\delta L_c(x)[n_c(x_0)-n_i]}{L_c(x_0)+\delta L_c(x)}. \tag{14}$$

For an accurate determination of $\delta n_c(x)$ it is necessary to know the interference orders in the coat region for both the interferograms, the geometry of the examined sample in the same region and the difference $(n_c(x_0)-n_i)$ of the refractive indices of the reference point in the coat and the immersion liquid, respectively.

Comparing Equations (10) and (7), it may be seen that their left hand sides are the same and thus the sets of fringes will be the same for the interferograms **1** and **2** in the region of coat, when the coat is uniform and when $n_i = n_c$. Then, for the interferogram **1** the set of interference fringes is continuous at the coat–immersion border. If, however, n_i differs from n_c but the coat of the examined object is uniform, we have from (7) and (10)

$$\delta L_c(x) = \frac{\lambda[\delta m_{1c}(x) - \delta m_{2c}(x)]}{(n_c - n_i)}. \tag{15}$$

Mismatching of the refractive indices of immersion and the uniform coat enables to determine the exact geometry of the examined object in the coat region when the value of mismatching is known, *i.e.* if we know the difference $n_c - n_i$. For a uniform object, Eq. (15) represents the relation between the interference orders of both the interferograms in the domain determined by the region of the uniform object.

Principal method. From the analysis carried out above, it follows that in order to find the distribution of the refractive index in the core (from (13)) two interferograms **1** and **2** must be produced to get the information about the interference orders in the core region. The absolute thickness of the examined object in the reference point $L(x_0)$ must be known, while from the other measurements the change of the thickness $\delta L(x)$ of the object in the core region must be determined (most conveniently along the scanning lines). The absolute thickness of the reference point can be measured for each scanning line separately or (if it is given for one principal scanning line passing through the reference point) the method of measurement and calculation of the thickness in the reference points on the remaining lines must be established. The method described is a principal method with the help of which the most accurate results may be obtained. It will be a basis for the approximate methods to be proposed below. First, however, the simplifying possibilities will be considered.

2.3. Thickness measurements

2.3.1. Principal method – the mechanical measurements

In order to calculate exactly refractive index distribution, the geometry of the examined object must be known. In accordance with the analysis carried out in this work, the expressions for thickness $L(x)$ in the arbitrary place have been divided into those for the thickness of the object in the reference point $L(x_0)$ and for the relative changes of the thickness $\delta L(x)$, where $L(x) = L(x_0) + \delta L(x)$. The measurement of the thickness distribution is somewhat troublesome. In practice, it suffices to perform the thickness measurement with an optimeter in several points, which under assumption of continuity of the surface allows us to make calculations in the knots of the scanning network as it has been described above in the principal method.

2.3.2. Interference measurement from two interferograms

Since, as we showed, the distribution of the thickness changes in a uniform coat can be calculated from the analysis of the interference orders we present the approximate methods of calculation. In practice, these methods simplify significantly the measurements. Obviously, the absolute thickness of the object in one reference point of the principal scanning line should be measured using another method (optimeter, micrometer gauge, *etc.*). Equation (15) may be used in some of the approximate methods.

If we assume for a moment that also the core is uniform and of the same refractive index as the coat $n = n_c$, the set of fringes visible in the coat would be visible in the core as well. From this set (given the difference $n_c - n_i$) changes of the slice thickness in the region of core could be calculated from the formula

$$\delta L(x) = \frac{\lambda[\delta m_{1c}^{*}(x) - \delta m_2(x)]}{n_c - n_i}. \tag{16}$$

In contrast to this, in the case of nonuniform core the set of fringes in the core region is different. Note that the coat region surrounds that of the core. Thus, knowing the fringes in the region of coat, we can determine them approximately in the core. The asterisk associated with interference orders in (16) means that what counts here are not the real orders visible in the core but rather the ones which are obtained in the region of core as a result of the said approximation (Fig. 6a). Thus, the asterisk means that the approximation of the $m(x)$ function have been done, this function being based on the data described by the indices of interference fringes. As a result of this approximation, the interference orders in the domain of the core are calculated. The thickness distribution (16) is obtained with the accuracy depending on: the ac-

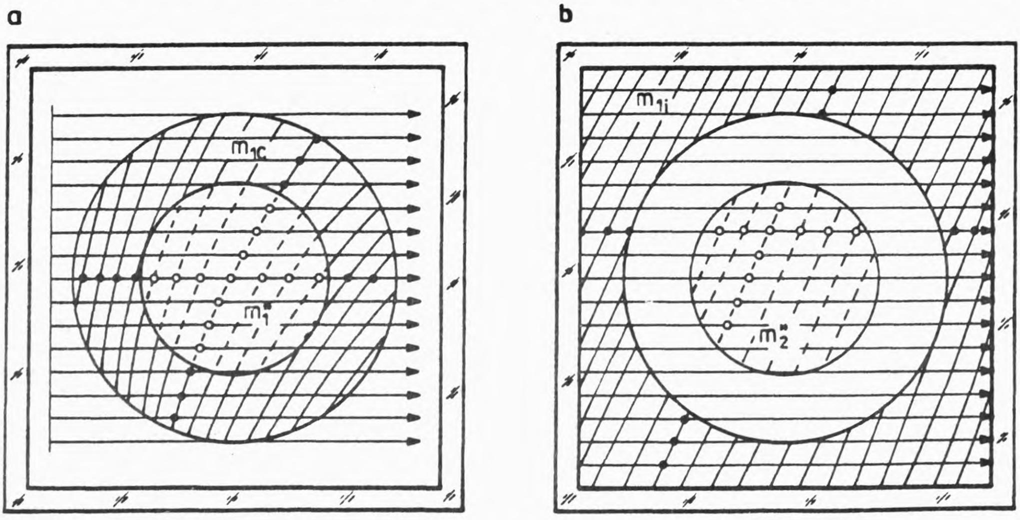

Fig. 6. Determination through extrapolation of the supposed sets of fringes m_1^* (a) and m_2^* (b). From the interferogram 1 the orders of interference (white circles) are found based on known position of orders (black circles). Two ways are shown – along the scanning lines and along the interference fringes

curacy of approximation carried out, the precision of the surfaces of the examined object and on the coat-to-core areas ratio. The calculation of m^*_{1c} in the core region may be performed with the help of different methods. It may be an approximation carried out for each scanning line separately, based on the data concerning the position of fringes (in the coat region) on the same scanning line. It may be also the approximation carried out separately for each fringe. The data for the approximation of the fringe positions are then collected from many lines in the coat region. The position of this fringe is calculated after determining its intersection points with the scanning lines.

2.3.3. Interference measurement from one interferogram

Previously, we took advantage of two interferograms during calculation of the thickness distribution. Since the regions of immersion and coat surround the core, the interference orders in the core may be calculated from the interferogram 1 by suitably extrapolating the fringes from both the coat and the immersion (Fig. 6). The orders of interference in the coat due to their extrapolation to the core region give the values of δm^*_{1c} (as previously). The orders from the immersion region due to their extrapolation to the core region give δm^*_{1i}. Equation (15) then takes the form

$$\delta L(x) = \frac{\lambda[\delta m^*_{1c}(x) - \delta m^*_{1i}(x)]}{(n_c - n_i)}. \tag{17}$$

The way of approximation (extrapolation) may be different as it has been described earlier. The data necesary for the approximation may be collected from the suitable regions along the scanning lines or along the interference fringes, *i.e* from different scanning lines.

Due to the relatively great distance of the immersion region, relatively large core region and unknown quality of the surface of the subject examined the degrees of the approximating polynomials should be very low (max. third degree). Then the probability of good approximation of the real course of the thickness distribution in the core region will be the highest. For significant simplifications the approximating polynomial may be reduced to the first one. Note that here we have to do with extrapolation rather than approximation.

2.3.4. Case without the measurement of the thickness distribution

A drastic simplification is to assume that the thickness of the examined object is stable ($\delta L(x) = 0$). This is admissible only for relatively thick objects. This case will be considered in more detail later on.

2.4. Analysis of the interference orders

2.4.1. Accurate analysis of the interferograms according to the principal method

Equation (13) allows us to determine in an accurate way the refractive index distribution in the core even when the quality of optical elements of both the interferometer and the cuvette is poor. Then the interferograms **1** and **2** are needed together with an additional measurement of the thickness distribution (the latter done by another method). By carrying out the analysis of the interferograms **1** and **2** in the region of the core in order to calculate $\delta n(x)$ from (13) no simplification is applied. This is the principal measurement method.

2.4.2. Analysis of one interferogram

In order to calculate $\delta n(x)$ from (13) only one interferogram is necessary. Having produced the interferogram 1 and carrying out the approximation (extrapolation) of the interference orders from the immersion region to the core region, we obtain δm_{1i}^{*} in the same way as it was the case for simplified measurement of the thickness ditribution. When exploiting the simplified analysis of the interferogram **1** only, Eq. (13) takes the form

$$\delta n(x) = \frac{\lambda[\delta m_1(x) - \delta m_{1i}^{*}(x)] - \delta L(x)[n(x_0) - n_i]}{L(x_0) + \delta L(x)}. \tag{18}$$

This is a simplified method.

2.4.3. Simplified method of single interferogram

The other approximation is suitable for the case of such positioning of the interference fringes that the fringes in the immersion region are maximally broadened and when it is reasonable to assume that in the core region $\delta m_{1i}^{*}(x) = 0$. This simplifies correspondingly Eq. (18).

2.5. Measurement of $n_c - n_i$

In the above given relations there appears the difference $n_c - n_i$. For a uniform coat $n(x_0) = n_c$. The difference $n_c - n_i$ of the refractive indices in the uniform coat and the immersion makes the measurement sometimes more difficult and sometimes easier (as it is the case when the thickness distribution of a uniform object is determined). In order to realize the measurement of $\delta n(x)$ and $\delta L(x)$ the said difference must be measured in the same measuring setup or using the same measurement method, which assures good accuracy. In the principal method, the measurements described in Subsections 2.5.1 and 2.5.2 are applied.

2.5.1. Measurement with a refractometer

The refractometric measurement consists in direct measurement of the refractive index of the coat n_c of the examined object as well as that of the immersion liquid n_i with the help of a refractometer. The lateral side of the coat of the examined object must be slightly ground to enable the entrance of the light to the coat, when the object is measured by the refractometer.

2.5.2. Immediate interference measurement of the $n_c - n_i$ difference

The difference $n_c - n_i$ may be measured by exploiting the examined slice which is usually of the wedge shape (Fig. 7) and has a uniform coat. In this case, however, the

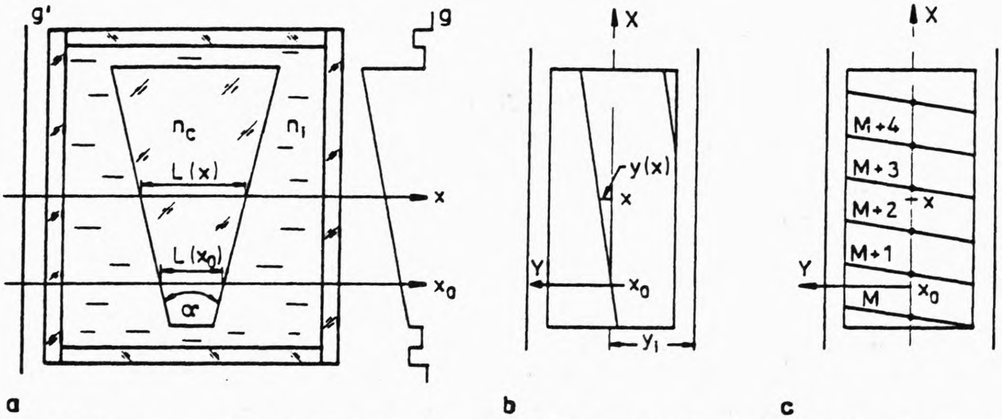

Fig. 7. Measurement of $n_c - n_i$ when a uniform coat of the examined object and a special wedge are exploited. **a** – section through the cuvette, **b** – for the rare fringes $\delta M_c(x) = y(x)/y_i$, **c** – for the dense fringes $\delta M_c(x) = m(x) - m(x_0)$

measurement of the absolute thickness must be performed in two points – in the coat region ($L_c(x_0)$ and $L_c(x)$). These points must be marked in the coat in such a way that the measurement of the interference orders δM_c in the coat region could be measured between these points. For calculation of $n_c - n_i$ the following dependence is used

$$n_c - n_i = \frac{\lambda \delta M_c(x)}{\delta L_c(x)} \tag{19}$$

where $\delta M_c(x)$ is a relative interference order, while $\delta L_c(x)$ is a relative thickness difference of the slice in the coat region. The dependence (19) is true for maximal broadening of the fringes in the immersion region (uniform background, *i.e.* $\delta m_{1i}(x) = 0$).

For the destructive method, thin slices of the examined object are usually cut off a long object. If the long object is inserted in a cuvette filled with immersion liquid (the same as used for measurement of slices) as it is the case for nondestructive examinations (the symmetry of the object axis being positioned perpendicularly to light beam in the interferometer), we get a setup for measuring the difference $n_c - n_i$ (Fig. 8**a**). Such a measurement is then possible to perform in the same interferometer. The interference fringes in the immersion region are set perpendicularly to the axis of the examined object (Fig. 8**b**). As it may be easily shown [11], [12] in the zero order approximation we have

$$n_c - n_i = \frac{\lambda \delta M_c(x)}{2\sqrt{R^2 - x^2}} \tag{20}$$

where $r_c \leqslant |x| \leqslant R$, r_c and R are the radii of the core and coat, respectively. The most accurate measurement will occur when the measurement of the relative interference order is performed for the coordinate x in the vicinity of the core. This method is the most convenient since it enables a direct measurement of $n_c - n_i$ in the same interferometer.

In a particular case when we have to do with a uniform bar (of the same refractive index as that of the coat), *i.e.* an object without core ($r_c = 0$), then

$$n_c - n_i = \frac{\lambda \delta M_c(x=0)}{2R} \tag{21}$$

where $\delta M_c(x=0)$ is (maximal) relative change of the interference order along the bar symmetry axis.

When measuring $n_c - n_i$, the most convenient way is to choose the reference point of the coat–immersion border. The measurement of the relative change of the interference order δM_c in the region of uniform coat can be made using the method of deviation of the fringes from rectilinearity (Fig. 7**b** and Fig. 8**b**) or the approximation method (Fig. 7**c** and Fig. 8**c**). For a small optical path differences

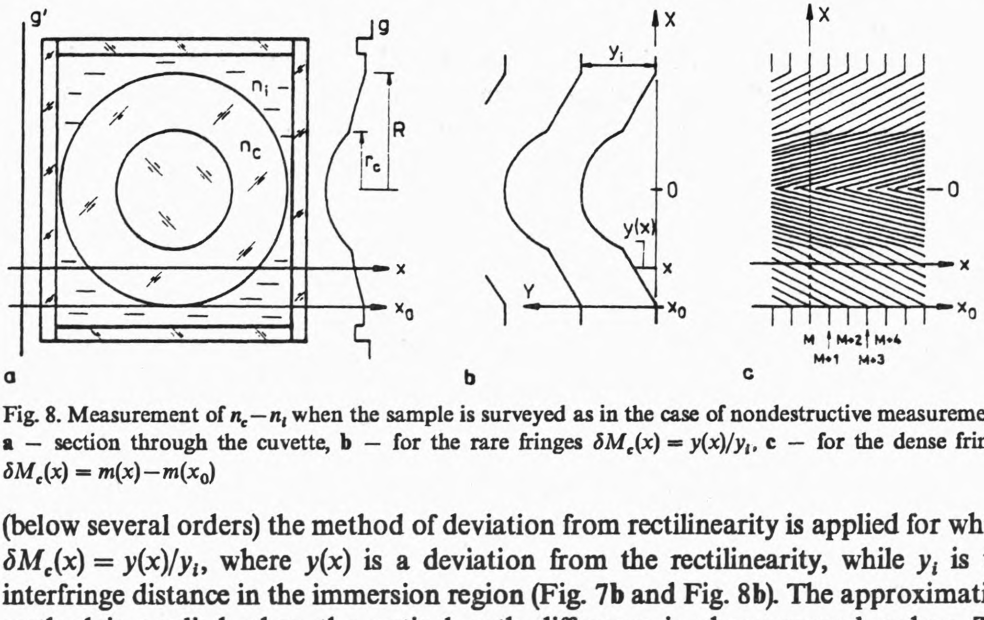

Fig. 8. Measurement of $n_c - n_i$ when the sample is surveyed as in the case of nondestructive measurements, **a** – section through the cuvette, **b** – for the rare fringes $\delta M_c(x) = y(x)/y_i$, **c** – for the dense fringes $\delta M_c(x) = m(x) - m(x_0)$

(below several orders) the method of deviation from rectilinearity is applied for which $\delta M_c(x) = y(x)/y_i$, where $y(x)$ is a deviation from the rectilinearity, while y_i is the interfringe distance in the immersion region (Fig. 7**b** and Fig. 8**b**). The approximation method is applied when the optical path difference is above several orders. The interference M orders are approximated as well as their position on the scanning line (Fig. 7**c** and Fig. 8**c**). From the approximation the relative order $\delta M_c(x)$ for an arbitrary x (in the region of the coat) is calculated. Instead of approximation we may apply an immediate measurement of $\delta M_c(x)$, evidently, with less accuracy.

2.5.3. Independent measurement of n_c and n_i

As such a measurement also a refractometric measurement may be employed. Here, the mixed method will be presented. If we have no long object of the refractive index n_c equal to that of the coat of the examined object, it is most convenient to perform an indirect measurement. To measure n_i a bar of known refractive index

n_c' is used and the formula (21) applied in which instead of n_c the index n_c' appears. The bar of the refractive index n_c' and of the known radius R may be inserted to the cuvette and we measure $\delta M(x=0)$. From (21) we calculate n_i. Instead of the uniform bar a uniform wedge of the refractive index n_c' may be used (Fig. 7). Equation (19) will have the form

$$n_c' - n_i = \frac{\lambda \delta M(x)}{2\delta x \tan(\alpha/2)} \tag{22}$$

where α is a wedge angle. Hence we calculate n_i. The above result is true when the fringes in the immersion liquid are set perpendicularly to the uniform wedge edge or when the fringes in the immersion region are maximally broadened (uniform background, *i.e.* $\delta m_{1i}(x) = 0$). For the high differences $n_c' - n_i$ the fringes in the wedge may be set arbitrarily (Fig. 7c) but in the liquid they should be maximally broadened (uniform background). The measurement of n_c of the examined object may be carried out in a refractometer as it was the case in Subsection 2.5.1.

2.5.4. Simplified measurement

Such a measurement consists in assuming that $n_c - n_i = 0$ in the formulae for δn from Subsection 2.2. If, in order to determine $\delta n(x)$, the thickness distribution is necessary and when an interference method is used to the latter, we must measure $n_c - n_i$. If the value of the difference $n_c - n_i$ is small, the accuracy of thickness distribution determination by the interference method (in accordance with Subsection 2.3.2) may be insufficient. In order to determine the thickness distribution, n_c being known, we may apply an arbitrary fluid of known refractive index and thus of high value of $n_c - n_i$. When the objects are thick and the difference $n_c - n_i$ is small usually the approximation that $n_c - n_i = 0$ is assumed. The measurement of the thickness distribution is then usually neglected ($\delta L(x) = 0$). The due analysis may be useful to determine conditions under which such a simplification is justified.

2.6. Analysis of the expressions for δn and simplified versions of the measurements

On the basis of the modifications of the principal method described above, we may state that to determine the refractive index distribution in the core, the knowledge of the thickness distribution of the examined sample in the core region as well as that of $n_c - n_i$ is necessary in addition to the analysis of interferograms. Let us assume that an arbitrary method described in Section 2.5 is applied to determine $n_c - n_i$ and this method will be of interest only so far as the measurement accuracies are concerned. This will be the only criterion for selection of this method for different modifications of the principal method. In Table 1 we give the formulae for the refractive index distribution for the introduced modifications and simplifications of the principal method. These modifications include: analysis of one or two interferograms, the way of determining the thickness distribution and two cases when the refractive indices of the coat and immersion are different and equal, respectively. The dependences in Tab. 1 contain the magnitudes following from the interference measurement of the thickness distribution.

Table 1. Dependence of $\delta n(x)$ for different measurements variants

		Measurement method of thickness $\delta L(x)$ distribution	Analysis: Two interferograms accurate (13)	One interferogram medium accuracy (18)	Simplified (13) when $\delta m_2(x) = 0$ or (18) when $\delta m^*_{1l}(x) = 0$
$n_c \neq n_l$	1	Mechanical	$\boxed{\delta n(x) = \dfrac{\lambda[\delta m_1(x)-\delta m_2(x)]-\delta L(x)(n_c-n_l)}{L(x_0)+\delta L(x)}}$	$\boxed{\delta n(x) = \dfrac{\lambda[\delta m_1(x)-\delta m^*_{1l}(x)]-\delta L(x)(n_c-n_l)}{L(x_0)+\delta L(x)}}$	$\delta n(x) = \dfrac{\lambda\delta m_1(x)-\delta L(x)(n_c-n_l)}{L(x_0)+\delta L(x)}$
	2	From two interferograms	$\delta n(x) = \dfrac{\lambda[\delta m_1(x)-\delta m^*_{10}(x)]}{L(x_0)+\lambda\dfrac{\delta m^*_{1c}(x)-\delta m_2(x)}{n_c-n_l}}$		
	3	From one interferogram		$\delta n(x) = \dfrac{\lambda[\delta m_1(x)-\delta m^*_{1c}(x)]}{L(x_0)+\lambda\dfrac{\delta m^*_{1c}(x)-\delta m^*_{1l}(x)}{n_c-n_l}}$	$\delta n(x) = \dfrac{\lambda[\delta m_1(x)-\delta m^*_{1c}(x)}{L(x_0)+\lambda\dfrac{\delta m^*_{1c}(x)}{n_c-n_l}}$
$n_c = n_l$	4	Simplified $\delta L(x)$	$\delta n(x) = \dfrac{\lambda[\delta m_1(x)-\delta m_2(x)]}{L(x_0)}$	$\delta n(x) = \dfrac{\lambda[\delta m_1(x)-\delta m^*_{1l}(x)}{L(x_0)}$	$\delta n(x) = \dfrac{\lambda\delta m_1(x)}{L(x_0)}$
	5	Mechanical or $\delta L(x)$ determined by another method	$\delta n(x) = \dfrac{\lambda[\delta m_1(x)-\delta m_2(x)]}{L(x_0)+\delta L(x)}$	$\delta n(x) = \dfrac{\lambda[\delta m_1(x)-\delta m^*_{1l}(x)]}{L(x_0)+\delta L(x)}$	$\delta n(x) = \dfrac{\lambda\delta m_1(x)}{L(x_0)+\delta L(x)}$

3. Measurement results

The measurement methods described above have many variants. The results presented here are only an illustration. An exemplified interferogram is presented in Fig. 9, and the measurement results – in Fig. 10. The measurements were carried out in a Mach–Zehnder interferometer [3], ($\lambda = 632.8$ nm). The reults presented concern the case in which only a linear compensation of wedge of the examined sample was performed ($\delta L(x)$ assumed to be linear on the basis of the thickness measurement in three points in the coat region).

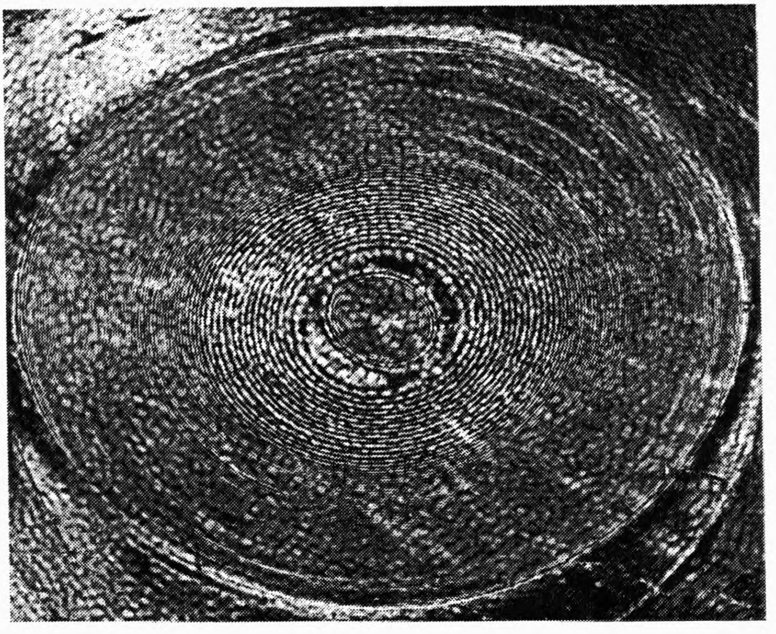

Fig. 9. Example of an interferogram of a preform slice ($L(x_0) = 2.43$ mm)

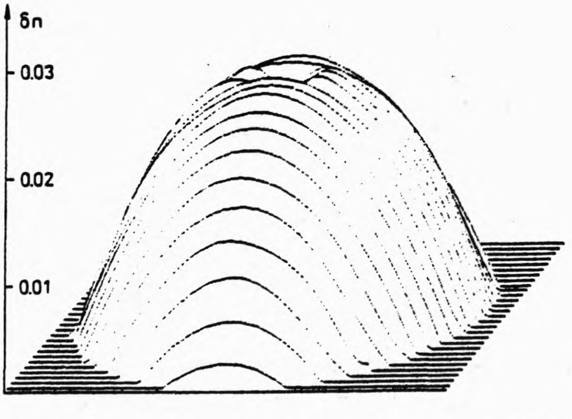

Fig. 10. Refractive index distribution in the exemplified preform slice

4. Analysis of the measurement accuracy

The measurement accuracies depend above all on the measurement method and the simplifications applied to both measurements and calculations. We shall analyse first the accuracies of determination of interference orders, $n_c - n_l$ differences, and thickness distribution measurements.

4.1. Accuracy of the interference orders distribution

In order to determine the measurement accuracies first the domain in which the interference measurements are possible will be determined. From (13) we have

$$\delta m_1(x) - \delta m_2(x) = \frac{\delta n(x)[L(x_0) + \delta L(x)]}{\lambda} - \frac{\delta L(x)(n_c - n_l)}{\lambda}. \tag{23}$$

The difference of the interference orders between two interferograms is composed of two fractions. The first one on the right hand side describes the influence of the refractive index nonuniformity $\delta n(x)$ in the examined region, while the other one describes the influence of its geometry $\delta L(x)$ and the mismatching of the refractive indices $n_c - n_l$. And thus for $\lambda = 632.8$ nm, for instance, and for $\delta n(x) = 0.01$ the first fraction takes the values given below.

$L(x_0)$ [mm]	$\delta L(x)$ [mm]				
	0.0001	0.001	0.01	0.1	1
0.01	0.16	0.17	0.32	1.74	15.96
0.1	1.58	1.60	1.74	3.16	17.38
1	15.80	15.82	15.96	17.38	31.61
10	158.03	158.04	158.19	159.61	173.83

For $\delta n(x)$ higher (or lower) by one order of magnitude these magnitudes increase (decrease) also by one order of magnitude.

The second fraction for the same wavelength takes the values given below.

	$\delta L(x)$ [mm]				
$n_c - n_l$	0.0001	0.001	0.01	0.1	1
0.0001	0.000	0.000	0.002	0.016	0.158
0.001	0.000	0.002	0.016	0.158	1.580
0.01	0.002	0.016	0.158	1.580	15.803
0.1	0.016	0.158	1.580	15.803	158.03

The optimal fringe density is equal to 20–40 in the examined region. For fringes distributed more densely or more rarely the relative errors increase slightly and must be accounted during the due analysis. Let us assume that the optimal difference

$\delta m_1(x) - \delta m_2(x)$ is about 10 (this value may be changed significantly). Note also that the fringe density in both the interferograms may be influenced by bending the mirrors of the interferometer. The edges of the two wedges generating the optical path difference may be on the same side of the interferometers or on the opposite sides. The components of Eq. (23) may have the same or opposite signs (influence of $\delta n(x)$, $\delta L(x)$, $n_c - n_i$). There is a number of possibilities and the range of the domain of the orders measurements is not quite strictly limited. From the immediate comparison of the components of Eq. (23), it may be seen which conditions must be fulfilled to eliminate the influence of the thickness difference of the examined object (the second component is small compared to the first one).

The accuracy of determination of the interference orders depends above all on the applied method of the interferogram analysis and to a less degree on the interference fringe density and the measuremental conditions. For an optimal density of interference fringes, the absolute error determination of the relative interference order $\sigma(\delta m(x))$ is equal to: 0.1–0.05 for visual measurements, and 0.01–0.005 for the measurements with the scanning device. In the present paper, the orders with asterisk occur, as well. They concern the extrapolation (approximation) of the interference orders from one region (either coat or immersion) to the other (core). Both the regions are separated while the first surrounds the other. The accuracies of the interference order determination in this case are less. They are limited by both the way the extrapolation (approximation) is performed and the number of data available for approximation. The error of the order $\delta m^*_{1c}(x)$ is influenced predominantly by the way the processing of the sample surface is carried out. The errors $\delta m^*_{1i}(x)$ (as well as $\delta m^*_{1c}(x)$) are influenced by the shape of the surfaces of the interferometer mirrors, interferometer beam splitters (and cuvette) and by the uniformity of the splitters (and cuvette). The errors of this kind are, as a rule, less, since the quality of the mentioned elements is high. For the order $\delta m^*_{1i}(x)$ the errors are slightly greater than for $\delta m^*_{1c}(x)$. This follows from the fact that the domain of the immersion data region is more distant from the sought domain of the core than the domain of the coat region. It may be assumed that for optimal density of the interference fringes the absolute error $\sigma(\delta m^*_{1c}(x))$ amounts to: from 0.5 to 02 for the visual method and from 0.2 to 0.1 for the scanning device. Similarly, the absolute error $\sigma(\delta m^*_{1i}(x))$ is: from 0. 2 to 0.1 for the visual method and from 0.1 to 0.05 for the scanning device.

4.2. Accuracy of the difference $n_c - n_i$ determination

4.2.1. Refractometric measurements

The measurements of the refractive indices n_c and n_i are made individually with the aid of a refractometer. The accuracies depend on the class of the refractometer. For high accuracies, the measuring conditions must be accounted. The measurements of n_c and n_i should be made at the same temperature in which the measurements of $\delta n(x)$ and $\delta L(x)$ are performed. This is especially important for the immersion liquid. It may be assumed that for typical measurements $\sigma(n_c) = 0.0001$ and $\sigma(n_i) = 0.0002$. The error of the refractive index difference amounts to $\sigma(n_c - n_i) = 0.0003$.

4.2.2. Direct interference measurement of n_c-n_l

The interference measurement of the difference n_c-n_l with the help of a wedge (examined slice) is described by the relation (19), from which we obtain the error

$$\left|\frac{\sigma(n_c-n_l)}{(n_c-n_l)}\right| = \left|\frac{\sigma(\lambda)}{\lambda}\right| + \left|\frac{\sigma(\delta M_c(x))}{\delta M_c(x)}\right| + \left|\frac{\sigma(\delta L_c(x))}{\delta L_c(x)}\right|. \tag{24}$$

The first component of the sum may be neglected, since it is very small for the laser light. The second component, for optimal density of the fringes (about 20–40 in the examined region) amounts to: 0.0025 for the visual method and 0.00025 for the scanning device. For the method of fringe deviation from rectilinearity this value is higher and for $\delta M_c(x) = 1$ is as high as the absolute error of the interference order determination $\sigma(\delta M_c(x))$. The third component depends on the device used to measure the absolute thickness of the examined object and on the thickness of this object. As it may be seen (from Subsection 4.3), the last component, for optimal fringe density, has a decisive influence on the relative error of the n_c-n_l difference measurement. This error takes the values given below.

	$\sigma(n_c-n_l)/(n_c-n_l)$				
$\sigma(\delta L_c(x))$ [mm]	$\delta L_c(x) = 0.001$ [mm]	$\delta L_c(x) = 0.01$ [mm]	$\delta L_c(x) = 0.1$ [mm]	$\delta L_c(x) = 1$ [mm]	$\delta L_c(x) = 10$ [mm]
			Visual scanning		
0.0001	0.1	0.0125	0.0035	0.0026	0.00251
0.001	1	0.1	0.0125	0.0035	0.0026
0.01	10	1	0.1	0.0125	0.0035
			Scanning device		
0.0001	0.1	0.01	0.00125	0.00035	0.00026
0.001	1	0.1	0.01	0.00125	0.00035
0.01	10	1	0.1	0.01	0.00125

For the method of interference fringe deviation from rectilinearity the values in the above table are correspondingly higher. The absolute error depends on the value of the measured n_c-n_l difference, and on the relative error from the above table.

For the measurement of the difference with the help of a bar (21) of diameter $2R$ the whole above analysis, including formula (23), is correct however, $\delta L_c(x)$ should be replaced by $2R$ and $\sigma(\delta L_c(x))$ by $\delta(2R)$.

4.2.3. Independent measurement of n_c and n_l

Interference measurement of n_l is a relative measurement for the known value of n'_c. In the final analysis the measurement accuracy for n'_c-n_l (as it was the case in Subsection 4.2.2) as well as the accuracy of $\sigma(n'_c)$ and $\sigma(n_c)$ must be accounted, i.e. $\delta(n_c-n_l) = \sigma(n'_c-n_l)+\sigma(n'_c)+\sigma(n_c)$. For intance, in order to determine n_l

a bar of known refractive index n_c' and diameter $2R = 10$ mm, $\sigma(2R) = 0.05$ mm and $\sigma(n_c') = 0.0001$ is applied. From the visual measurements we have, according to formula (21), $n_c' - n_i = 0.001$. Hence, $\sigma(n_c' - n_i) = [0.0025 + 0.05/10]0.001 = 7.5 \cdot 10^{-6}$, and thus this error is negligible. From the refractometric measurement we know n_c with the accuracy $\sigma(n_c) = 0.0001$. Hence, $\sigma(n_c - n_i) = \sigma(n_c' - n_i) + \sigma(n_c') + \sigma(n_c) = 0.0002$.

4.3. Accuracy of the thickness distribution measurement

The errors of the absolute thickness measurement $L(x_0)$ are the same as those described in Subsection 4.3.1, since these are mechanical measurements. The errors of the thickness distribution measurements will be described below.

4.3.1. Mechanical measurement

These errors depend on the devices applied. Such devices may be: optimeter ($\sigma(L(x_0)) = 0.001$ mm), micrometer gauge ($\sigma(L(x_0)) = 0.01$ mm), or special electronic gauges ($\sigma(L(x_0)) = 0.0001$ mm). The thickness distribution is estimated by measuring the thickness in many points. The errors of thickness distribution would be twice that of a single thickness measurement since $\delta L(x) = L(x) - L(x_0)$. As we make an approximation (which smoothes the results of measurements), the error of the thickness distribution becomes slightly less. This depends on the shape of the measured sample and on the density of the data taken to the approximation. In practice, however, it can be assumed that the error of the thickness distribution measurement is the same as that of a single measurement.

4.3.2. Interference measurement from two interferograms

From the analysis of (16) we get

$$\left|\frac{\sigma(\delta L(x))}{\delta L(x)}\right| = \left|\frac{\delta(\lambda)}{\lambda}\right| + \left|\frac{\sigma[\delta m_{1c}^*(x) - \delta m_2(x)]}{\delta m_{1c}^*(x) - \delta m_2(x)}\right| + \left|\frac{\sigma(n_c - n_i)}{n_c - n_i}\right|. \tag{25}$$

The first component on the right hand side of this equality may be neglected. The second component, when assuming the optimal fringe density and when the denominator amounts to about 10 and for the data from Subsection 4.1, is equal to: $0.06 - 0.025$ for the visual method, and $0.021 - 0.01$ for the scanning device. The third component depends on the applied measurement method (Subsect. 4.2). The method may be chosen in such a way that this component be small as compared to the second one. Thus, it may be seen at once which requirements for the measurements should be imposed to receive the required accuracy. For example, if a scanning device is used for the measurements when $\delta L_c(x) = 0.1$ mm and $\sigma(\delta L_c(x)) = 0.001$ mm, the relative measurement error of the thickness distribution ranges between 0.0725 and 0.0375.

4.3.3. Interference measurement from a single interferogram

From the analysis of (17) we obtain the dependence identical with (25). The only thing to do is to replace $\delta m_2(x)$ by $\delta m_{1i}^*(x)$. The whole analysis will be the same as that in Subsection 4.3.2 but the second component, when $\delta m^{*}_{1c}(x) - \delta m^{*}_{1i}(x) = 10$, will amount to: 0.07–0.03 for the visual method, and 0.03–0.015 for the scanning device.

4.4. Accuracy of the refractive index distribution

In Table 1 the dependences for the refractive index distribution both for the principal method and for the derivative simplified methods are shown. Comparing these dependences, it may be seen immediately what the simplifications consist in, and thus the errors may be easily calculated. The dependences for the principal methods are given in the frames. The remaining dependences describe the derivative (simplified or modified) methods. Below, we shall give the dependences describing the relative errors of the methods. These errors will be calculated from the dependence

$$\sigma(\delta n(x)) = \Sigma A_i. \tag{26}$$

4.4.1. Principal method

From the analysis of (13) we obtain:

$$\begin{aligned}
A_1 &= \left|\frac{\delta m_1(x) - \delta m_2(x)}{L(x_0) + \delta L(x)}\right| \sigma(\lambda),\\
A_2 &= \left|\frac{\lambda}{L(x_0) + \delta L(x)}\right| [\sigma(\delta m_1(x)) + \sigma(\delta m_2(x))],\\
A_3 &= \left|\frac{\delta L(x)}{L(x_0) + \delta L(x)}\right| [\sigma(n_c(x_0)) + \sigma(n_i)],\\
A_4 &= \left|\frac{\delta n(x)}{L(x_0) + \delta L(x)}\right| \sigma(L(x_0)),\\
A_5 &= \left|\frac{-(n_c - n_i) - \delta n(x)}{L(x_0) + \delta L(x)}\right| \sigma(\delta L(x)).
\end{aligned} \tag{27}$$

For the interference measurement methods for the thickness distribution, the errors $\sigma(\delta L(x))$ may be calculated from the dependence (25) and $\sigma(\delta n(x))$ from (27), respectively. Taking advantage of the dependences given in Tab. 1 (for the measurement of $\delta L(x)$ from the interferograms), the errors may be calculated which for the analysis of two interferograms (and the dependence in Tab. 1, line 2) are equal to:

$$\begin{aligned}
A_1 &= \left|\frac{\delta n(x) L(x_0)}{\lambda B}\right| \sigma(\lambda),\\
A_2 &= |\lambda/B| \sigma(\delta m_1(x)),\\
A_3 &= \left|\frac{\delta n(x)\lambda}{(n_c - n_i)B}\right| \sigma(\delta m_2(x)),\\
A_4 &= \left|\frac{[-1 - \delta n(x)]\lambda}{(n_c - n_i)B}\right| \sigma(\delta m^{*}_{1c}(x)),
\end{aligned}$$

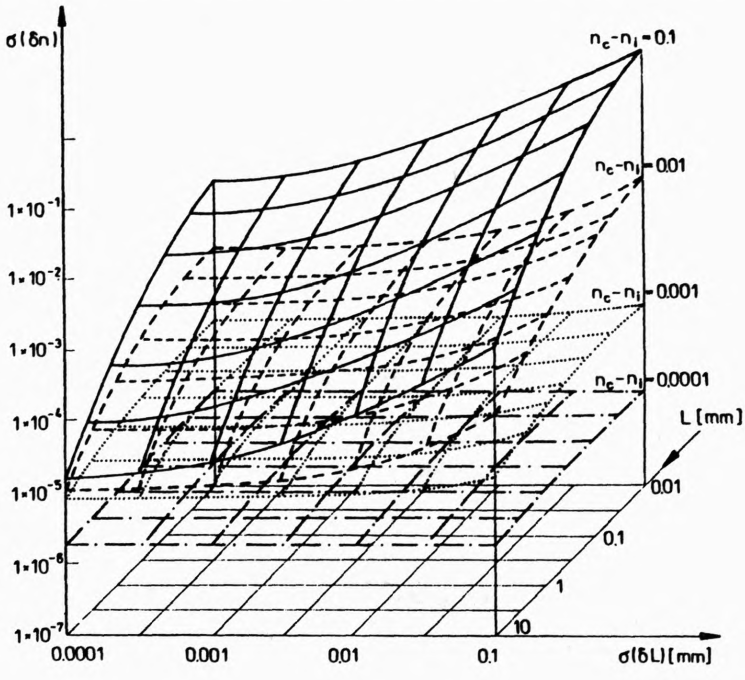

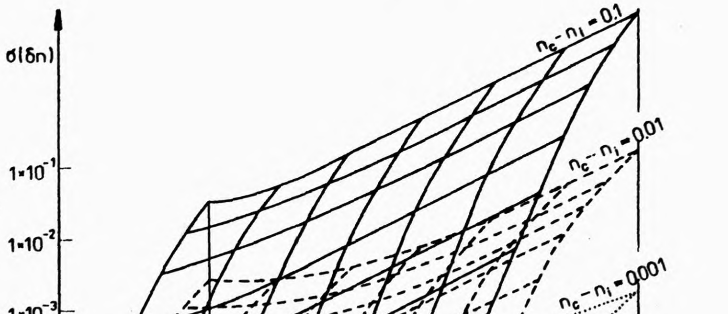

Fig. 11. Absolute error of the refractive index distribution measurement $\sigma(\delta n)$ for the principal method. The error calculated according to (27) under assumption that $\sigma(L) = 2\sigma(\delta L)$, $\delta m_1 - \delta m_2 = 10$, $\lambda = 632.8$ nm, $\sigma(n_c)+\sigma(n_l) = 0.0003$. The logarithmic scale. **a** – visual method $\sigma(\delta m_1 - \delta m_2) = 0.2$, **b** – method with the scanning device $\sigma(\delta m_1 - \delta m_2) = 0.02$

Table 2. Absolute $\sigma(\delta n)$ and relative $\sigma(\delta n)/\delta n$ and percentage contributions of the error components ($\Delta m = \delta m_1(x) - \delta m_2(x)$)

$\delta L = 0.001$ mm			$\sigma(\delta m) = 0.1$							$\sigma(\delta m) = 0.01$						
$\sigma(\delta L)$ [mm]	Δm	$L(x_0)$ [mm]	$\sigma(\delta n)$	$\frac{\sigma(\delta n)}{\delta n}$ [%]	Error components [%]					$\sigma(\delta n)$	$\frac{\sigma(\delta n)}{\delta n}$ [%]	Error components [%]				
					A_1	A_2	A_3	A_4	A_5			A_1	A_2	A_3	A_4	A_5
			$n_c - n_l = 0.1$; $\sigma(n_c - n_l) = 0.01$							$n_c - n_l = 0.1$; $\sigma(n_c - n_l) = 0.01$						
0.001	1	0.01	0.03032	62.6	0.0	37.9	3.0	14.5	44.5	0.019966	41.2	0.0	3.8	4.5	22.0	67.6
		0.1	0.00245	46.4	0.0	51.2	4.0	2.1	42.6	0.001320	25.0	0.1	9.5	7.5	4.0	79.0
		1	0.000237	44.6	0.0	53.2	4.2	0.2	42.3	0.000124	23.2	0.1	10.2	8.1	0.4	81.2
		10	0.000024	44.4	0.0	53.5	4.2	0.0	42.3	0.000012	23.2	0.1	10.3	8.1	0.0	81.4
	10	0.01	0.12454	22.0	0.1	9.2	0.7	41.3	48.6	0.114184	20.2	0.1	1.0	0.8	45.1	53.0
		0.1	0.003573	5.8	0.2	35.1	2.8	17.1	44.8	0.002445	4.0	0.4	5.1	4.0	25.0	65.4
		1	0.000250	4.0	0.4	50.6	4.0	2.5	42.5	0.000136	2.2	0.7	9.3	7.3	4.6	78.0
		10	0.000024	3.8	0.4	53.0	4.2	0.3	42.1	0.000012	2.0	0.8	10.1	8.0	0.5	80.6

Table 2 continued

$\delta L = 0.001$ mm			$\sigma(\delta m) = 0.1$							$\sigma(\delta m) = 0.01$						
$\sigma(\delta L)$ [mm]	Δm	$L(x_0)$ [mm]	$\sigma(\delta n)$	$\frac{\sigma(\delta n)}{\delta n}$ [%]	Error components [%]					$\sigma(\delta n)$	$\frac{\sigma(\delta n)}{\delta n}$ [%]	Error components [%]				
					A_1	A_2	A_3	A_4	A_5			A_1	A_2	A_3	A_4	A_5
			$n_c - n = 0.001$; $\sigma(n_c - n_l) = 0.0001$							$n_c - n_l = 0.001$; $\sigma(n_c - n_l) = 0.0001$						
0.001	1	0.01	0.02206	38.4	0.0	52.2	0.0	23.7	24.1	0.0117	20.4	0.1	9.8	0.1	44.6	45.4
		0.1	0.001389	22.2	0.1	90.2	0.1	4.5	5.2	0.000261	4.2	0.4	48.0	0.4	23.7	27.5
		1	0.000129	20.4	0.1	98.1	0.1	0.5	1.3	0.000015	2.4	0.7	83.7	0.7	4.2	10.8
		10	0.000013	20.2	0.1	99.0	0.1	0.0	0.8	0.0000014	2.2	0.7	90.5	0.7	0.4	7.6
	10	0.01	0.11627	20.2	0.1	9.9	0.0	45.0	45.0	0.10592	18.4	0.1	1.1	0.0	49.4	49.4
		0.1	0.002514	4.0	0.4	49.8	0.0	24.7	25.1	0.001386	2.2	0.7	9.0	0.1	44.7	45.4
		1	0.000141	2.2	0.7	89.6	0.1	4.5	5.2	0.000027	0.4	3.6	46.2	0.4	23.1	26.7
		10	0.000013	2.0	0.8	97.4	0.1	0.5	1.3	0.0000016	0.3	6.2	79.0	0.6	3.9	10.2
0.0001	1	0.01	0.012577	21.9	0.1	91.5	0.1	4.1	4.2	0.002222	3.9	0.4	51.8	0.4	23.5	23.9
		0.1	0.001268	20.3	0.1	89.8	0.1	0.5	0.6	0.000141	2.2	0.7	89.1	0.7	4.4	5.1
		1	0.000127	20.1	0.1	99.7	0.1	0.0	0.1	0.000013	2.1	0.8	96.7	0.8	0.5	1.2
		10	0.000013	20.1	0.1	99.7	0.1	0.0	0.1	0.0000013	2.0	0.8	97.6	0.8	0.0	0.8
	10	0.01	0.02207	3.8	0.4	52.1	0.0	23.7	23.7	0.011717	2.0	0.8	9.8	0.1	44.6	44.7
		0.1	0.001389	2.2	0.7	90.2	0.1	4.5	4.5	0.000261	0.4	3.8	48.0	0.4	23.7	24.1
		1	0.000129	2.0	0.8	98.1	0.1	0.5	0.6	0.000015	0.2	6.6	83.7	0.7	4.2	4.8
		10	0.000013	2.0	0.8	98.9	0.1	0.0	0.1	0.0000014	0.2	7.1	90.5	0.7	0.4	1.2

$$A_5 = \left|\frac{\delta n(x)\lambda[m^*_{1c}(x)-\delta m_2(x)]}{(n_c-n_i)^2 B}\right|\sigma(n_c-n_i),$$

$$A_6 = |-\delta n(x)/B|\sigma(L(x_0)), \tag{28}$$

where

$$B = L(x_0)+\frac{\lambda[\delta m^*_{1c}(x)-\delta m_2(x)]}{n_c-n_i}.$$

Dependences (27) concern analysis for two interferograms. For analysis of one interferogram, the two dependences become the same. The only thing is to replace $\delta m_2(x)$ by $\delta m^*_{1i}(x)$. This dependence is rather complex. It is most convenient to draw up the tables of measurement accuracies, according to which the suitable measuring conditions are selected. Table 2 contains a small fragment of such a large table of errors. Figure 11 illustrates the absolute errors of refractive index distribution measurements. These errors illustrate the influence of the most essential factors upon the measurement accuracies. These factors are: n_c-n_i, $L(x_0)$, $\sigma(\delta L(x_0))$, $\sigma(L(x_0))$.

4.4.2. Derivative methods

The most accurate measurement method (of those discussed in this paper) is the method of analysis of two interferograms and with mechanical or interference measurement of the geometry $\delta L(x)$ of the examined sample. Below we are going to discuss successive simplifications which introduce more and more significant measurement errors:

1. Simplified analysis of two interferograms (when $\delta m_2(x) = 0$) with mechanical or interference measurement of $\delta L(x)$.

2. Analysis of a simple interferogram with mechanical or interference measurement of $\delta L(x)$.

3. Simplified analysis of single interferogram (when $\delta m^*_{1i}(x) = 0$) with interference measurement of $\delta L(x)$.

4. Simplified analysis of either two interferograms or a single interferogram when the measurement of $\delta L(x)$ concerns only the linear factor.

5. Assumption (for calculations) that $n_c-n_i = 0$ when this difference is small.

6. Simplified analysis of either two interferograms or a single interferogram when the measurement of sample geometry is neglected, i.e. $\delta L(x) = 0$.

Ad 1, 2. The errors are calculated from (27) or (28). It is assumed that $\delta m_2(x) = 0$ and the error $\sigma(\delta m_2(x))$ is estimated visually depending on the quality of both cuvette and interferometer.

Ad 3. For the method of single interferometer analysis, the dependences are the same as that described by (28) but the term $\delta m_2(x)$ should be replaced by $\delta m^*_{1c}(x)$.

Ad 4. If the measurement of geometry $\delta L(x)$ refers only to the linear factor, the analysis of errors is the same as that given by (27) or (28), but the errors of geometry measurements $\sigma(\delta L(x))$ may approach the half of the maximal change of the thickness difference for the estimated sample (in the examined region).

Ad 5. The exploitation of the dependence given in Tab. 2, line 5, for $n_c = n_i$ (then $n_c - n_i = \sigma(n_c - n_i)$) leads to errors, which for analysis of two interferograms are as follows:

$$A_1 = |\delta n(x)/\lambda| \sigma(\lambda),$$

$$A_2 = \left|\frac{\delta n(x)}{\delta m_1(x) - \delta m_2(x)}\right| [\sigma(\delta m_1(x)) + \sigma(\delta m_2(x))],$$

$$A_3 = \left|\frac{-\delta n(x)}{L(x_0) + \delta L(x)}\right| [\sigma(L(x_0)) + \sigma(\delta L(x))],$$

$$A_4 = \left|\frac{-\delta L(x)\sigma(n_c - n_i)}{L(x_0) + \delta L(x)}\right|,$$

$$A_5 = \left|\frac{A_4}{\delta L(x)} - \frac{A_4}{L(x_0) + \delta L(x)}\right| \sigma(\delta L(x)),$$

$$A_6 = \left|\frac{-A_4}{L(x_0) + \delta L(x)}\right| \sigma(L(x_0)),$$

$$A_7 = \left|\frac{-\delta L(x)}{L(x_0) + \delta L(x)}\right| \sigma(n_c - n_i). \qquad (29)$$

Ad 6. The neglection of the thickness distribution measurements results in drastic simplifications (dependence in Tab. 2, line 4), which is independent of $n_c - n_i$ and $\delta L(x)$ and the errors of which become

$$A_1 = |\delta n(x)/\lambda| \sigma(\lambda),$$

$$A_2 = \left|\frac{\delta n(x)}{\delta m_1(x) - \delta m_2(x)}\right| [\sigma(\delta m_1(x)) + \sigma(\delta m_2(x))],$$

$$A_3 = |-\delta n(x)/L(x_0)| \sigma(L(x_0)),$$

$$A_4 = \left|\frac{-\delta L(x)[(n_c - n_i) + \delta n(x)]}{L(x_0) + \delta L(x)}\right|,$$

$$A_5 = \left|\frac{-\delta n(x)\delta L(x)/\lambda}{L(x_0) + \delta L(x)}\right| \sigma(\lambda),$$

$$A_6 = \left|\frac{-\lambda \delta L(x)/L(x_0)}{L(x_0) + \delta L(x)}\right| [\sigma(\delta m_1(x)) + \sigma(\delta m_2(x))],$$

$$A_7 = \left|\frac{-\delta L(x)}{L(x_0) + \delta L(x)}\right| \sigma(n_c - n_i),$$

$$A_8 = \left|\frac{-L(x_0)[(n_c - n_i) + \delta n(x)]}{[L(x_0) + \delta L(x)]^2}\right| \sigma(\delta L(x)),$$

$$A_9 = \left| \frac{\delta L(x)[(n_c - n_i) + \delta n(x)(2 + \delta L(x)/L(x_0))]}{[L(x_0) + \delta L(x)]^2} \right| \sigma(L(x_0)). \tag{30}$$

The components A_4 in dependences (29) and (30) represent the errors introduced by the assumed simplifications. These errors have a decisive influence on the final measurement errors and decide practically whether the assumed simplifications can satisfy the required measurement accuracies. In Figure 12, the values of the components A_4 are shown. Thus, from Fig. 12 or from the formulae for A_4 the conditions can be determined, under which the measurement based on such

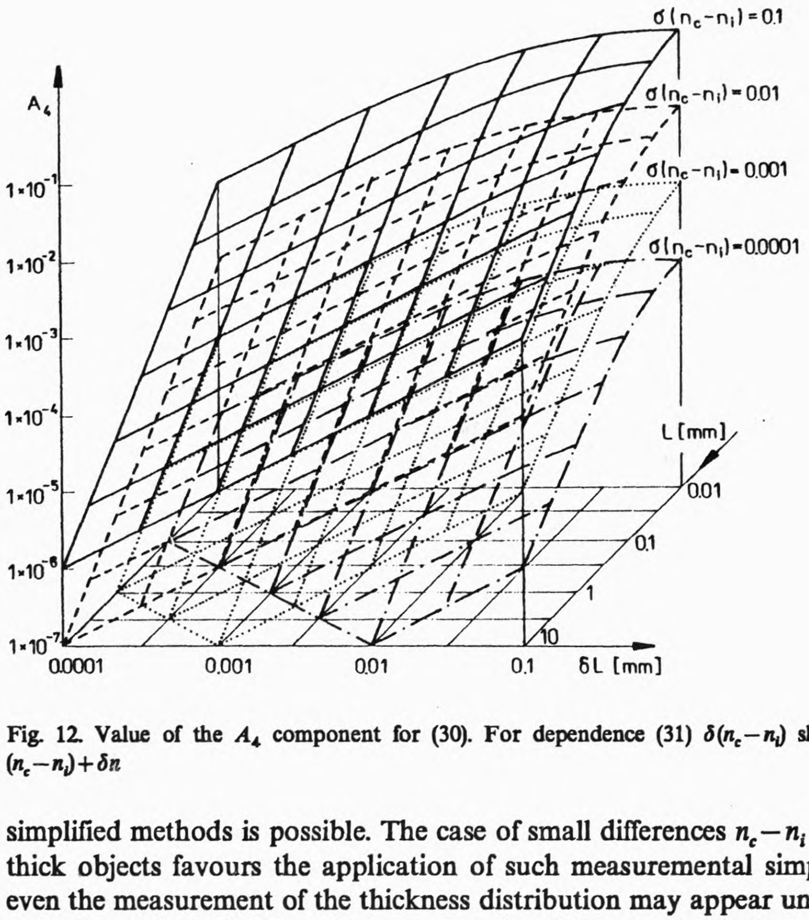

Fig. 12. Value of the A_4 component for (30). For dependence (31) $\delta(n_c - n_i)$ should be replaced by $(n_c - n_i) + \delta n$

simplified methods is possible. The case of small differences $n_c - n_i$ and the relatively thick objects favours the application of such measuremental simplifications. Then, even the measurement of the thickness distribution may appear unnecessary. On the other hand, if we decide not to measure the thickness distribution, the measurement of $n_c - n_i$ becomes unnecessary on the basis of formulae for $\delta n(x)$. From the formulae for A_4 it may be seen that in order to diminish A_4 the refractive index n_i must be chosen in such a way that the condition $n_c - n_i = -\delta n_{max}/2$ is fulfilled, where δn_{max} is the maximal value of $\delta n(x)$. For such radical simplifications the conditions, for which the total error of the measurement (including the error of simplification) is still admissible, may be established on the basis of (29) and (30).

5. Concluding remarks

During the measurement of the refractive index distribution in the slices of preforms or light waveguides the most important factors influencing of the measurement accuracies are: thickness distribution of the slice examined and the difference of the refractive indices $n_c - n_l$. The measurement of these magnitudes makes the measurements slightly more complex and therefore they have been discussed in this work extensively. The accuracy analysis carried out together with the described variants and simplifications of the measurement allows us to select the optimal measurement method. This is the method selected on the basis of the admissible measurement error and simultaneously on admissible simplifications of the method. These simplifications, especially those concerning the measurement of the thickness distribution, give significant economic advantages reducing also the time consumption. These advantages are especially important when many measurements are carried out. This work has been done just for the latter case.

References

[1] Kowalik W., Dubik B., SPIE, **670** (1986), 73.
[2] Kowalik W., Dubik B., Pietraszkiewicz K., Płokarz H., SPIE **670** (1986), 77.
[3] Kowalik W., Michalski M., SPIE **670** (1986), 82.
[4] Kowalik W., Dubik B., SPIE **1085** (1989), 319.
[5] Kowalik W., Dubik B., SPIE **1085** (1989), 328.
[6] Kowalik W., Dubik B., SPIE **1085** (1989), 333.
[7] Vest C. M., Appl. Opt. **14** (1975), 1601.
[8] Kokubun Y., Iga K., Appl. Opt. **19** (1980), 846.
[9] Sochacki J., Appl. Opt. **25** (1986), 3473.
[10] Kowalik W., Heimrath A., SPIE **670** (1986), 68.
[11] Kowalik W., Dubik B., Opt. Appl. **20** (1990), 3.
[12] Kowalik W., Dubik B., Opt. Appl. **20** (1990), 17.
[13] Kowalik W., Dubik B., Opt. Appl. **20** (1990), 33.
[14] Kowalik W., Dubik B., Opt. Appl. **20** (1990), 45.
[15] Kowalik W., Appl. Opt. **17** (1978), 2956.

Received January 4, 1993